Theoretical studies of the Earth's ionosphere inhomogeneities influence on the propagation of HF radio waves

Andrew S. Kryukovsky[1], Dmitry S. Lukin[1], Eugene A. Palkin[1], Eugene B. Ipatov[2] and Dmitry V. Rastyagaev[1]

[1] Russian New University, 22, Radio Street, Moscow, 105005, Russian Federation
[2] Moscow Institute of Physics and Technology, 9, Institutsky per., Dolgoprudny, 141700, Russian Federation
`rdv@rosnou.ru`

Abstract. In the article algorithms for studying the characteristics of frequency-modulated (FM) radio signals reflected from the ionosphere containing local plasma inhomogeneities is studied. Mathematical simulation of vertical sounding ionograms for various inhomogeneities both in the case of an ordinary wave as well as in the case of an extraordinary wave is carried out by the method of Hamilton-Lukin bi-characteristics. An algorithm for mathematical modeling of LFM HF radio signals propagation in a magnetically active ionospheric plasma is considered. The algorithm is based on a multipath description of the received HF signal, the amplitude-phase characteristics of the components of which are determined on the basis of the extended bi-characteristic system. The proposed method is focused on predicting the polarization characteristics taking into account the geometry of the inclined trajectories of the probing rays. On the basis of the bi-characteristics method, an algorithm recovering the effective frequency of electron collisions in the ionosphere, using data on signal attenuation during vertical sounding of the ionospheric plasma with a continuous frequency-modulated decameter signal has been developed. The results of numerical simulation are presented. The work is of an overview nature. The study was supported by a grant from the Russian Science Foundation (project No. 20-12-00299).

Keywords: ionosphere, irregularities, ionograms, ordinary and extraordinary waves, vertical sounding, bi-characteristic system, effective frequency of electron collisions, polarization characteristics, Stokes parameters.

1   Introduction

Diagnostics and monitoring of the ionosphere, permanent monitoring of extreme phenomena in the atmosphere are the urgent tasks due to the significant influence of the state of the ionosphere on the operation of radio systems for various purposes: radio communication, navigation (positioning), radar, etc. The efficiency of the systems of short-wave radio communication and radio navigation depends on an adequate de-

scription of the propagation medium taking into account all sufficient processes in the ionosphere.

The most promising method for solving this problem is mathematical modeling of the propagation of radio waves in a disturbed ionospheric plasma, connected directly to the operational data of oblique and vertical sounding. Vertical sounding (VS) ionosondes are one of the most effective diagnostic tools for the ionosphere with a long history of development [1].

The ray-tracing method is one of the efficient mathematical modeling methods for the radio waves propagation problems. But when studying the propagation of HF radio waves by ray methods, the problem of describing fields in the caustics arises. The relevance of the study of caustic structures is determined by their special role with respect to ray structures, since caustics, which are the envelopes of ray families, divide the physical space into regions with different propagation patterns [2]. We also note that the field in the vicinity of the caustic increases substantially. So the diffraction-ray approach to the description of HF waves propagation in the ionosphere is used, and it gives the possibilities to describe as regular ray field structures, so as diffraction field structures in the caustics regions.

Here we shall consider the wave field structure in the vicinity of the caustic near the Earth's surface without taking into account the radio waves reflected from the surface, but taking into account the absorption and divergence of the radio signal in the ionospheric anisotropic plasma. We shall consider the polarization characteristics of HF signals at the receiving point in the diffraction-ray approach.

2 Extended bi-characteristic system for describing the parameters of a short-wave signal in a magnetically active ionospheric plasma

Based on diffraction-ray approach the description of HF waves propagation in the ionosphere reposes on a Hamiltonian system of ordinary differential equations (ODE) for the spatial coordinates of the rays $\vec{r} = (x, y, z)$, the component of the wave vectors $\vec{k} = (k_x, k_y, k_z)$ and on the concomitant system of ODE for the partial derivatives that definer the geometric divergence of radiation fluxes in the coordinate-momentum space (in the space coordinates and wave vectors) [3; 4]:

$$\frac{dr_i}{dt} = \left(\frac{c^2}{\omega} k_i - \frac{\omega}{2} \frac{\partial \varepsilon}{\partial k_i} \right) \left(\varepsilon + \frac{\omega}{2} \frac{\partial \varepsilon}{\partial \omega} \right)^{-1}$$

$$\frac{dk_i}{dt} = \frac{\omega}{2} \frac{\partial \varepsilon}{\partial r_i} \left(\varepsilon + \frac{\omega}{2} \frac{\partial \varepsilon}{\partial \omega} \right)^{-1} \quad i = 1, 2, 3,$$

(1)

$$\frac{d\vec{r}_\theta}{dt} = \frac{\partial}{\partial \theta}\left(\left(2c^2\vec{k} - \frac{\partial \omega^2 \varepsilon}{\partial \vec{k}}\right)\bigg/\frac{\partial \omega^2 \varepsilon}{\partial \omega}\right)$$

$$\frac{d\vec{k}_\theta}{dt} = \frac{\partial}{\partial \theta}\left(\frac{\partial \omega^2 \varepsilon}{\partial \vec{r}}\bigg/\frac{\partial \omega^2 \varepsilon}{\partial \omega}\right)$$

$$\frac{d\vec{r}_\varphi}{dt} = \frac{\partial}{\partial \varphi}\left(\left(2c^2\vec{k} - \frac{\partial \omega^2 \varepsilon}{\partial \vec{k}}\right)\bigg/\frac{\partial \omega^2 \varepsilon}{\partial \omega}\right)$$ (2)

$$\frac{d\vec{k}_\varphi}{dt} = \frac{\partial}{\partial \varphi}\left(\frac{\partial \omega^2 \varepsilon}{\partial \vec{r}}\bigg/\frac{\partial \omega^2 \varepsilon}{\partial \omega}\right)$$

With initial conditions for spatial coordinates in the report system associated with the radiation source, and components of wave vectors:

$$k_1(0) = k_x(0) = \frac{\omega}{c}\sqrt{\varepsilon_0}\cos\theta\cos\varphi,$$

$$k_2(0) = k_y(0) = \frac{\omega}{c}\sqrt{\varepsilon_0}\sin\theta\cos\varphi,$$ (3)

$$k_3(0) = k_z(0) = \frac{\omega}{c}\sqrt{\varepsilon_0}\sin\varphi,$$

$$r_1(0) = x(0) = x_0, \quad r_2(0) = y(0) = y_0, \quad r_3(0) = z(0) = z_0,$$

And corresponding initial conditions for partial derivatives with respect to the parameters of the ray family:

$$k'_{x\theta}(0) = -\frac{\omega}{c}\sqrt{\varepsilon_0}\sin\theta\cos\varphi, \quad k'_{x\varphi}(0) = -\frac{\omega}{c}\sqrt{\varepsilon_0}\cos\theta\sin\varphi,$$

$$k'_{y\theta}(0) = -\frac{\omega}{c}\sqrt{\varepsilon_0}\sin\theta\sin\varphi, \quad k'_{y\varphi}(0) = \frac{\omega}{c}\sqrt{\varepsilon_0}\cos\theta\cos\varphi,$$ (4)

$$k'_{z\theta}(0) = \frac{\omega}{c}\sqrt{\varepsilon_0}\cos\theta, \qquad k'_{z\varphi}(0) = 0.,$$

$$\vec{r}'_\theta(0) = 0, \qquad \vec{r}'_\varphi(0) = 0$$

The initial conditions (3-4) are set at the location of the radiation source on the Earth's surface, assuming that the influence of the ionosphere can be neglected at this level. In formulas (1-4), ω is the circular frequency of radiation, c is the speed of light, t is the parameter along the ray path and $\varepsilon(\vec{r},\vec{k},\omega)$ is the effective permittivity

of the wave propagation medium, which takes into account the properties of inhomogeneous magnetically active ionospheric plasma for two normal components of an electromagnetic wave (the "ordinary" and "extraordinary" wave components with circular polarization) [1,5].

Within the framework of approximation involved, if the deflecting influence of absorption is neglected, which is acceptable for the ionospheric plasma, then the expression for the effective permittivity has the form [1; 5]:

$$\varepsilon_{\pm} = 1 - \frac{2v(1-v)}{2(1-v) - u\sin^2\alpha \pm \sqrt{u^2\sin^4\alpha + 4u(1-v)^2\cos^2\alpha}} \tag{5}$$

The following notations are introduced in expression (5):

$$v = \left(\frac{\omega_{\mathrm{p}}}{\omega}\right)^2 = \frac{4\pi e^2 N(\vec{r})}{m_e \omega^2} \tag{6}$$

– ratio of the square of the plasma frequency to the square of the working frequency:

$$u = \left(\frac{\omega_H}{\omega}\right)^2 = \frac{e^2 H_0^2}{m_e^2 c^2 \omega^2} \tag{7}$$

– ratio of the square of the gyrofrequency to the square of the operating frequency.

In formulas (6) and (7), m_e is the mass of the electron, e is the charge of the electron, H_0 is the value of the magnetic field of the Earth, and the function $N(\vec{r})$ is the electron concentration at a fixed point in space.

In addition to the functions u and v, the angle α between the Earth's magnetic field strength $\vec{H}_0 = (H_{0x}, H_{0y}, H_{0z})$ and wave vector $\vec{k}$ enters into formula (5) too:

$$H_{0x} = H_0\cos\gamma\cos\varphi, \quad H_{0y} = H_0\cos\gamma\sin\varphi, \quad H_{0z} = H_0\sin\gamma \tag{8}$$

The orientation of the magnetic field is given by the angles γ and φ. When calculating, you only need to know $\cos^2\alpha$:

$$\cos^2\alpha = \frac{(H_{0x}k_x + H_{0y}k_y + H_{0z}k_z)^2}{H_0^2\left|\vec{k}\right|^2} \tag{9}$$

The sign "+" in formula (5) corresponds to an ordinary wave, and the sign "–" corresponds to an extraordinary wave (o-wave and an x-wave, respectively). To construct ray paths, we use the bi-characteristic system method, described above (see also [6–8]).

3 Ray trajectories calculation

As an example of the ray trajectory calculation algorithm we consider the following problem. Figure 1 shows the dependence of the electron concentration on height, and Figure 2 shows the dependence of the electron collision frequency [9; 17]. It is assumed that a monochromatic signal is emitted with an operating frequency $f = 3.3$ MHz.

To calculate the field in the vicinity of the caustic, a high-latitude night ionospheric plasma model corresponding to March, 80° North latitude and 30° Eastern longitude was used. The angle $\gamma = -83°$, the angle $\varphi = 90°$, $H_0 = 0{,}551$ Oe. We assume that the radiation source is point-wise and is located on the surface of the earth at the coordinate origin. Radiation of an electromagnetic wave occurs in the plane (x, z).
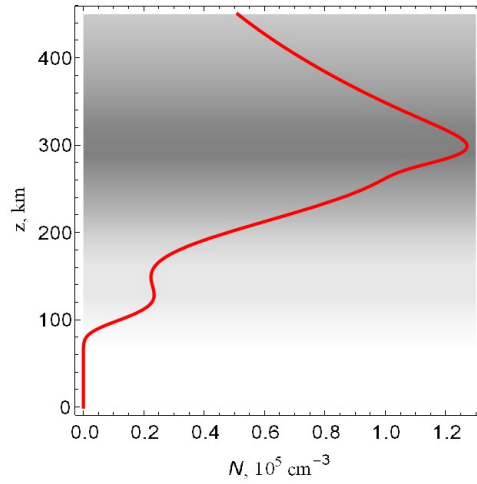

**Fig. 1.** Dependence of the electron concentration on height.
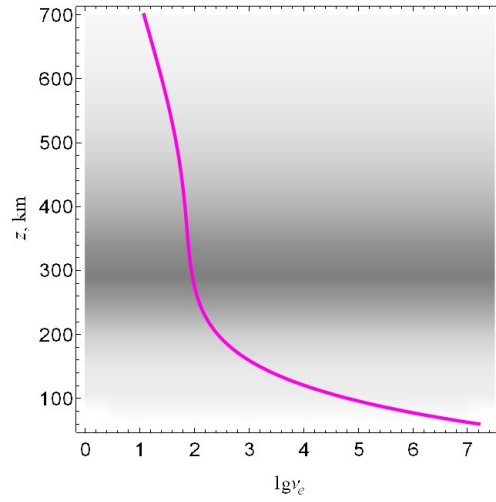
Fig. 2. Dependence of the electron frequency of collisions on height.

Figures 3 and 4 [17] show the ray structure of the radio signal in the (x, z) plane for an *o*-wave and an *x*-wave. The angle of the ray exit varies from 0° to 90°. As a background, as in Figure 1 and 2, the electron concentration of the ionosphere is shown. At an altitude of about 300 km, the maximum of the *F* layer is clearly visible, and at an altitude of 115 km the maximum of the *E* layer too. Rays corresponding to the propagation of an *o*-wave are reflected from the E and F layers with a small exit angle and return to the ground, and rays with large exit angles pass through the ionosphere.
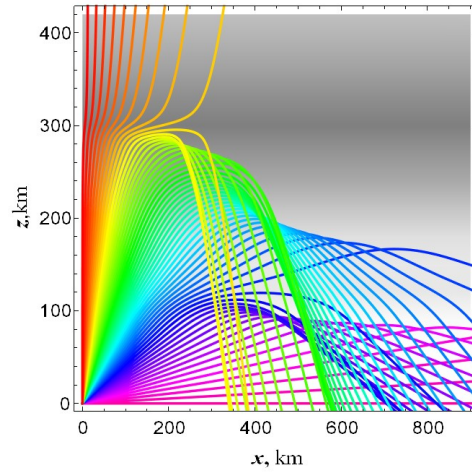
Fig. 3. Ray structures in the (x, z) plane, *o*-wave.
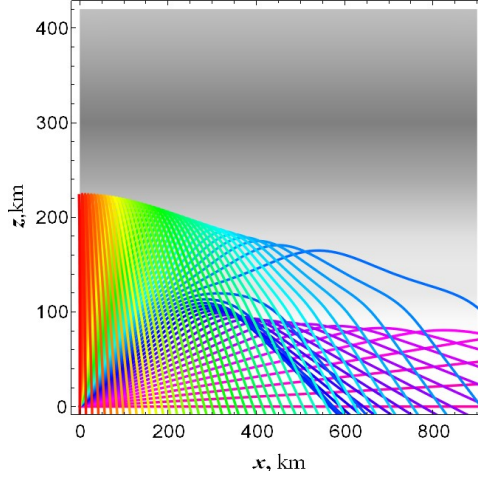
Fig. 4. Ray structures in the (x, z) plane, x-wave.

Figure 3 shows that the family of rays forms a complex caustic structure containing three caustic points. In accordance with the classification of wave catastrophe, this is a catastrophe of A_3 [7; 10]. The lower caustic cusp is caused by layer E, and the two upper caustic cusps are determined by ionospheric layers forming the main maximum.

In the case of an x-wave, all rays are reflected from the ionosphere and returned to the Earth. Part of the rays forms the upper caustic, and part of the rays with small exit angles form a caustic cusp, due to layer E. It can be seen that three lower branches of caustics, forming the A_3 singularities, descend to the earth at distances of 333.755 km, ~ 575 km and ~ 750 km [17]. The paper considers the structure of the wave field in the vicinity of the first caustic (yellow rays) without taking into account the surface wave, the effect of which is negligible in this conditions. According to Figure 4 there is an x-wave field that modulates the caustic field of an ordinary wave in this region too.

4 Wave field calculation

Let an isotropic radiation source create an electric field E_0 at a distance r_0. Then:

$$E_0 = \frac{\sqrt{30W}}{r_0} \quad (V/m). \tag{10}$$

In formula (10), W is the radiation power, and r_0 is the distance to the emitter. In this work, it was assumed that $W = 1\ kW$ and $r_0 = 1\ m$.

Then the wave field at the receiving point is formed as a result of coherent or incoherent addition of the partial fields of individual beams:

$$\vec{E}(\vec{r}_{rec},t) \cong \sum_{j=1}^{N} \vec{A}_j(\theta_j,\varphi_j,t) \exp\left\{i\left[\Phi(\theta_j,\varphi_j,t)+\omega t\right]\right\}\Big|_{\vec{r}_{rec}} \qquad (11)$$

Here N is the number of rays coming to the observation point; θ_j, φ_j – the angular coordinates of the output of the ray with the number j; falling at the location of the receiver, $\Phi(\theta_j,\varphi_j,t)$ - the phase path, $\vec{A}_j(\theta_j,\varphi_j,t)$ – the vector of the electric (magnetic) field of the wave corresponding to the j-th ray. In formula (11), the slow dependence of the field on time t, which occurs in the presence of non-stationary in-homogeneities in the ionosphere, is distinguished. It is also assumed that the reception of ionospheric reflected radiation occurs on the Earth's surface, that is, the influence of magnetically active plasma at the receiving point can be neglected.

As fallows from the ray structure analysis, the field of an o-wave to the right of the caustic is defined as the sum of the contributions of two rays:

$$E_g^o \cong A_1^o \cdot \exp\left(i\left(\Phi_1^o - \pi/2\right)\right) + A_2^0 \cdot \exp\left(i\Phi_2^0\right) \qquad (12)$$

The first ray has already touched the caustic, and the second is not yet. The radia-tion field of an x-wave in this region is single-ray:

$$E_g^x \cong A_1^x \cdot \exp\left(i\left(\Phi_1^x - \pi/2\right)\right) \qquad (13)$$

This ray has already touched the upper caustic. In formulas (12) – (13), the ampli-tude coefficients can be represented as:

$$A_j = E_0 \exp[-\psi_j]\sqrt{\left|\frac{J_0}{J_j}\right|} \qquad (14)$$

In expression (14), J_j is the Jacobian of the divergence calculated at the observa-tion point using the extended bi-characteristic system, J_0 is the Jacobian of the diver-gence calculated at a distance r_0 from the source, ψ_j is the absorption determined by the electron collision frequency, and Φ_j is the phase calculated like absorption, along the ray path [8]. In our notation, the first ray is the ray that has already touched the caustic.

Since the Jacobian J_j on the caustic is equal to zero due to ray focusing, solution (14) becomes infinite. Therefore, the field on the caustic and in its vicinity is deter-mined using uniform asymptotic through the Airy function and its derivative (see, for example, [7,11]):

$$E_c \cong \exp(i\theta)\left(l_1 \cdot Ai(\lambda) - i l_2 \cdot \frac{dAi(\lambda)}{d\lambda}\right) \qquad (15)$$

In expression (15):

$$Ai(\lambda) = \int\limits_{-\infty}^{+\infty} \exp\left(i\left(\xi^3 + \lambda\,\xi\right)\right)d\xi \tag{16}$$

Is the Airy function, θ is the phase of the traveling wave, and λ is the argument of the Airy function, which in the light region (where two rays intersect) are defined as:

$$\theta = \frac{1}{2}\left(\Phi_1 + \Phi_2\right), \quad \lambda = -\frac{3}{2^{4/3}}\left|\Phi_1 - \Phi_2\right|^{2/3} \tag{17}$$

The coefficients of the asymptotic expansion (15) l_1 and l_2 in a first approximation have the form:

$$l_1 \cong \frac{1}{2\sqrt{\pi}}\left(A_1 + A_2\right)\sqrt[4]{-3\lambda}, \quad l_2 \cong \frac{3}{2\sqrt{\pi}}\left(A_1 - A_2\right)\frac{1}{\sqrt[4]{-3\lambda}} \tag{18}$$

The problem of the field determination on the caustic and in its vicinity is due to the need to solve the "shooting" problem, that is, calculating with high accuracy at one point the phases and amplitudes of two rays that came along different but near trajectories. For the lower branches of the caustic, this task is especially time-consuming, since the caustic and the rays in its vicinity are quasi-parallel.

Another algorithm is inherently close to the method of interpolating local asymptotics [14] and is alternative to the local approach [15]. The angle of exit of the ray forming the caustic was initially calculated. Knowing this angle, the ray family in the vicinity of the caustic was divided into two subfamilies: a subfamily of rays that touched the caustic and did not touch it. Relative to each ray, the point of its intersection with the earth's surface and all the necessary radiation parameters at this point were determined. Then for each ray subfamily, the interpolation formulas for the phases and amplitude coefficients were constructed using the least squares method. Then the parameters of two intersecting rays were found at each point, and the radiation and caustic fields were calculated using the formulas given above.

Figure 5 [17] shows the ray amplitudes in the vicinity of the caustic in the ray approximation. The solid line shows the amplitudes of the rays of an o-wave that have not yet touched the caustics, and the dotted line – that have already touched. The position of the caustic is marked by a vertical red line. The dashed line shows the amplitudes of the x-wave.

In Figure 6 the amplitude of the field of an o-wave in the vicinity of the caustic is shown. Uniform asymptotics calculated by formulas using the Airy function and its derivative (15) are shown in black and blue colors [17].

The black color shows the calculations made taking into account the absorption, and the blue line shows the calculations without taking into account the absorption. The red dot on the horizontal axis shows the position of the caustic. The maximum value is shifted to the region of light relative to the position of the caustic as expected. On the caustic, the field amplitude is close in value to the average values of the field amplitude in the light region. In addition, this figure shows a comparison of the field amplitude on the caustic calculated using the uniform asymptotics (15) and the ray

approximation (12). The green color indicates the geometrical-optical (GO) approximation without taking into account absorption, and the purple color shows the approximation taking into account absorption. It should be noted that the GO approximation in the region of light very well coincides with uniform asymptotics up to the slopes of the main maximum.
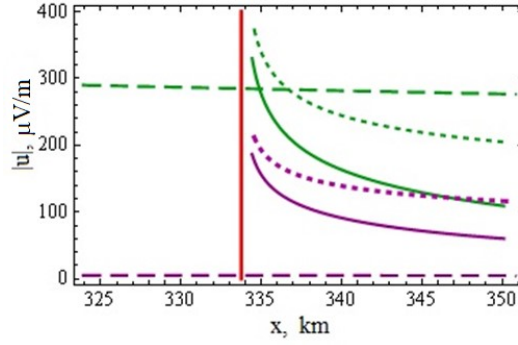

Fig. 5. The amplitudes of the rays in the vicinity of the caustic without taking into account absorption (green) and taking into account absorption (purple).

It follows from the figure that in order to estimate the maximum value of the field amplitude in the vicinity of the caustic using the ray approximation, it is enough to determine where the curve forms the inflection point before going to infinity.
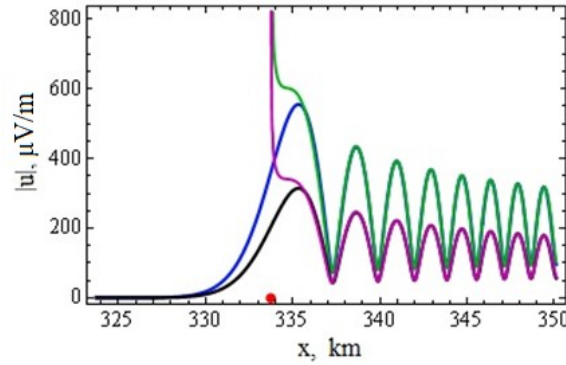
Fig. 6. The amplitude of the electric field intensity modulus versus the distance along the horizontal axis; *o*-wave.

Figure 7 shows the amplitudes of the field of an *o*-wave, taking into account the contribution of the *x*-wave in the vicinity of the caustic in the caustic, but excluding the absorption. We can see that the *x*-wave makes a significant contribution and strongly modulates the caustic structure of the *o*-wave [17].
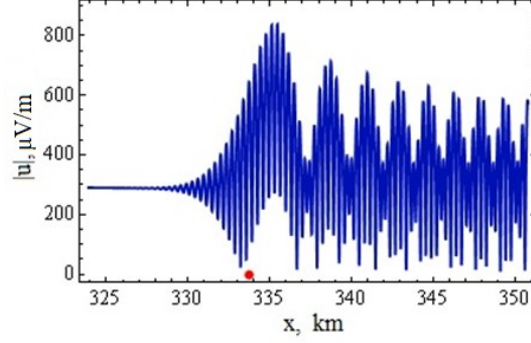
Fig. 7. The amplitude of the electric field strength modulus versus the distance along the horizontal axis without taking into account absorption, but taking into account the contribution of the *x*-wave.

5   Algorithm for calculating the polarization characteristics of HF signals at the receiving point

To calculate the polarization characteristics of HF signals at the receiving point we use the formula (11), where the total field is the result of coherent or incoherent addition of the partial fields of individual beams. It is also assumed that the diffraction effects due to the caustic regions are not presented at the receiving point.

In (11) it is necessary to determine coherently summing components and non-coherently summing ones, the fact taking into account that different components have different degrees of coherence, since they correspond to different trajectories of wave propagation through spatially separated regions of the inhomogeneous ionosphere. In this case, to determine the polarization characteristics, we use the Stokes parameter system [16]:

$$
\begin{aligned}
S_0 &= \sum_{j=1}^{N} \left\langle A_{x\,j}^2(\theta_j, \varphi_j, t) \right\rangle + \left\langle A_{y\,j}^2(\theta_j, \varphi_j, t) \right\rangle \Big|_{\vec{r}_{rec}} \\
\tilde{S}_1 &= \left[I_{x,\tilde{j}} - I_{\tilde{y}} \right]\Big|_{\vec{r}_{rec}}, \quad \tilde{S}_2 = \left[I_{45,\tilde{j}} - I_{45,\tilde{j}} \right]\Big|_{\vec{r}_{rec}}, \quad \tilde{S}_3 = \left[I_{O,\tilde{j}} - I_{H,\tilde{j}} \right]\Big|_{\vec{r}_{rec}}
\end{aligned}
\tag{19}
$$

In formula (19) $I_{x,\tilde{j}}, I_{y,\tilde{j}}, I_{45,\tilde{j}}, I_{-45,\tilde{j}}, I_{O,\tilde{j}}, I_{H,\tilde{j}}$ are respectively the intensity of the linear components of the field strength vector in the specified directions $x, y, 45^0, -45^0$, as well as the "ordinary" and "extraordinary" components of the waves measured for the coherent part of the total field. S_0 is the total intensity of the wave field at the receiver. In (19) the local coordinate system associated with the selected direction signal (orientation of main lobe of receiving antenna diagram) is used with respect to which the components x, y of vectors $\vec{A}_j(\theta_j, \varphi_j, t)$ so as the

"mixed" direction of linear polarization oriented at angles $\pm 45^0$ are determined. The number $\tilde{j}$ is determined by all the coherent components of the signal. In particular, in the model numerical calculations constructed for the corresponding models of the effective permittivity of ionospheric plasma, the components of the "ordinary" and "extraordinary" waves were used to calculate the coherent part of the Stokes parameters, providing they correspond to ray trajectories close in the exit direction. For simplicity, in the model calculations we assume that the corresponding components of the "ordinary" and "extraordinary" waves are completely coherent, while the modes corresponding to rays reflected from different ionospheric layers or local inhomogeneities are not coherent. It is also necessary to note that the partial depolarization of "ordinary" and "extraordinary" waves exists, that occurs when the direction of arrival of a transverse electromagnetic wave does not coincide with the main direction of reception in polarization measurements. In addition, if there is a significant (for the recording equipment used) difference in the signal arrival times for different modes, it is possible to determine the polarization characteristics for individual groups of recorded signals that correspond to different propagation paths in the ionosphere.

For example, figure 8 shows the results of modeling the frequency dependence of the main parameters of the multipath structure of the recorded signal, which allow us to construct the frequency dependence of the Stokes parameters [20]. Figure 8 shows the frequency dependence of the wave arrival angles φ_j relative to the local horizon at the receiving point at a distance of 350 km from the source and the intensity of different modes (normalized by the field intensity at a distance of 1 m from the source).

The data obtained allow us to determine the mode structure of the signal at different frequencies, which is necessary for polarization characteristics forecasting. The calculation was performed only in the geometrical-optical approximation, since the diffraction effects in the focal regions have significantly smaller scales of frequency variations.
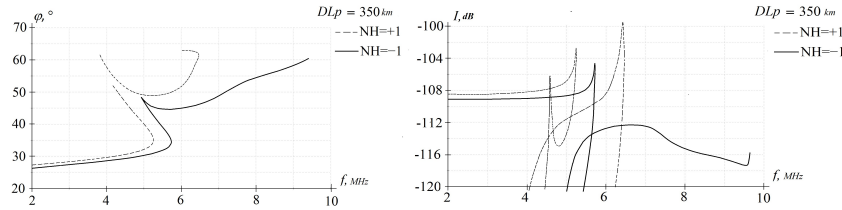
Fig. 8. Frequency dependence of the arrival angles and the intensity for different modes of the received signal (two branches of the graph respond to the "ordinary" (NH = -1) and "extraordinary " (NH = +1) components of the wave).

The graph in figure 9 shows the results of numerical prediction of the frequency dependence of the normalized Stokes parameter $S_3 = \tilde{S}_3 / S_0$ of the probing signal that characterizes the ratio of right-and left-polarized components in the total field at the receiving point [20]. When performing calculations, it was assumed that for each frequency value there is one dominant pair of coherent signal modes that have a maximum intensity of waves.

In the diffraction zones corresponding to the regions of spatial focusing of individual modes, a jump-like change in the mode structure occurs, which can be easily traced from the graph of figure 3. In these regions, there are small-scale oscillations of a diffraction nature. They are not shown in the graph.
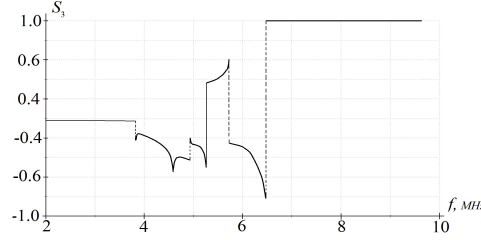
Fig. 9. Frequency dependence of the normalized Stokes parameter $S_3 = \tilde{S}_3 / S_0$ of the received signal.

6 Diagnostics of the effective frequency of electronic collisions in the ionosphere based on analysis of the amplitude characteristics of continuous LFM radio signals

Also, we consider an algorithm for determining the effective collision frequency based on the analysis of the amplitude characteristics of linear frequency modulated (LFM) signals [18]. When the chirp ionosonde is operating, the signal delay and amplitude are usually recorded depending on the radiation frequency (f). In this paper, the case of vertical sounding is considered. It is assumed that the electron density profile $N(z)$ as a function of the height z is known, that is, it has already been reconstructed from the dependence of the signal delay on the radiation frequency. As for the effective collision frequency, it should be reconstructed from the attenuation of the amplitude (A) of the probing signal, which can be represented in the form (11). Knowing the amplitude A, E_0 and the divergence D, we can proceed to determining the effective collision frequency in accordance with formula (11). Absorption along the path is defined as [3]:

$$\psi = -\frac{\omega}{2}\int_0^t \varepsilon_2 \, dt \qquad (20)$$

Formula (20) includes an approximate expression for the imaginary part of the dielectric constant of the medium having the form [3,8]:

$$\varepsilon_2 \cong -\nu Z \left(1+Z^2\right)^{-1}, \quad Z = \nu_e / \omega \qquad (21)$$

If we assume that the effective collision frequency at heights of the order of 80 km does not exceed 10^6 s^{-1}, then in (18) the denominator can be neglected, and it can be assumed that $\varepsilon_2 \approx -vZ$. Then, taking into account (21), equation on the energetic characteristics can be rewritten as:

$$\frac{V_c}{\omega^2}\int_0^{t_m} \nu_e N \, dt = L \qquad L = -\ln\frac{A}{D E_0} \qquad V_c = \frac{4\pi e^2}{m_e} \qquad (22)$$

In formula (22), L is a function of the operating frequency and is determined at the receiving point. t_m is a function of frequency too. This is the time it takes for the signal to travel from the source of the reflection point. As for ν_e and N, they are functions of the height z, which in turn are functions of the group time t, the function $z(t)$ is calculated along the trajectory and also depends on the frequency. Equation (22) is essentially Volterra integral equation of the second kind. One of the methods for solving it is the iteration method [18]. Let's introduce the notation: $G = \nu_e N$. We will assume that up to a certain frequency f_0, for which the time t_{m0},

$$\int_0^{t_{m0}} G \, dt = 0 \qquad (23)$$

We divide the frequency interval (f_0, f_{lev}) into n parts $(f_0, f_1,\ldots, f_j,\ldots, f_n = f_{lev})$, on each of which (with number j) we will assume the function G to be constant $(G = G_j)$. Let us calculate the values of t_{mj} as a function of frequency for each f_j. Then

$$G_1 = L_1 \frac{\omega_1^2}{t_{m1} - t_{m0}}, \quad G_2 = L_2 \frac{\omega_2^2}{t_{m2} - t_{m1}} - G_1 \frac{t_{m1} - t_{m0}}{t_{m2} - t_{m1}}$$

$$G_j = L_j \frac{\omega_j^2}{t_{m,j} - t_{m,j-1}} - \sum_{i=1}^{j-1} G_i \frac{t_{m,i} - t_{m,i-1}}{t_{m,j} - t_{m,j-1}}, \quad j \geq 2 \qquad (24)$$

Knowing the values of G_j and assuming that this is the product of the effective collision frequency of electrons and the electron concentration at the reflection point, it is easy to find the dependence of the effective collision frequency on height.

Below there is an example of the implementation of this algorithm using model calculations. In Figure 10 the dependence of the electron concentration on the height, and in Figure 11 effective collision frequency are shown [18].
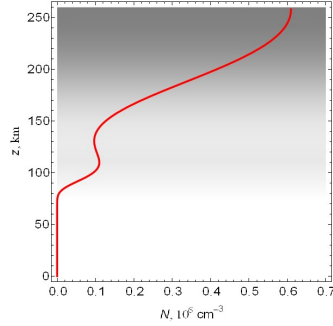
**Fig. 10.** Dependence of electron concentration on height.
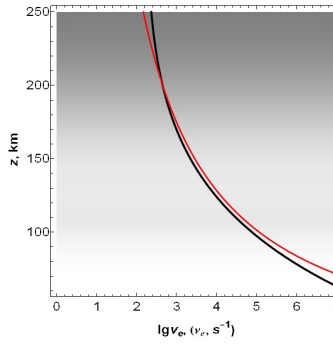
Fig. 11. Dependence of the logarithm of the collision frequency on the height.

It can be seen that a two-layer model has been selected (Figure 10). This structure of the ionosphere inevitably leads to the loss of data at some frequencies during vertical sounding (see also Figures 12-15). In Figure 11, the thin red line shows the approximation of the effective collision frequency by the hyperbolic dependence:

$$\lg \nu_e = a + b/z, \quad a = 0.217841, \quad b = 487.771 \tag{25}$$

which is typical for heights below the maximum of the $F2$ layer. The purpose of the simulation is to calculate the field amplitude at different frequencies at the receiving point from the known data, using the above formulas, and then, using the technique outlined above and formulas (24), (25) restore the effective collision frequency and compare model and calculated values.

Figure 12 shows the dependence of the signal reflection height on the frequency, calculated from the initial data [18]. In the region of 3 MHz, a gap is seen due to the interlayer valley. In Figure 13 the dependence of the time of arrival of the ray at the point of reflection on the frequency is shown [18]. A sharp increase in the curves in the region of the interlayer valley and the maximum of the $F2$ layer inevitably leads to instability of the iterative process when the effective collision frequency is restored.
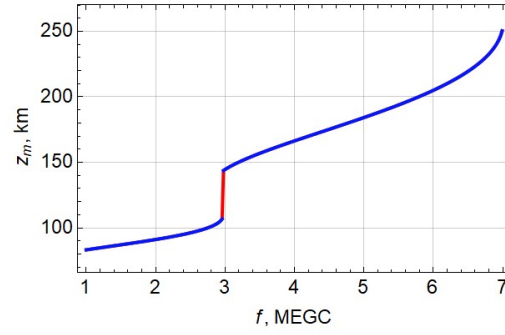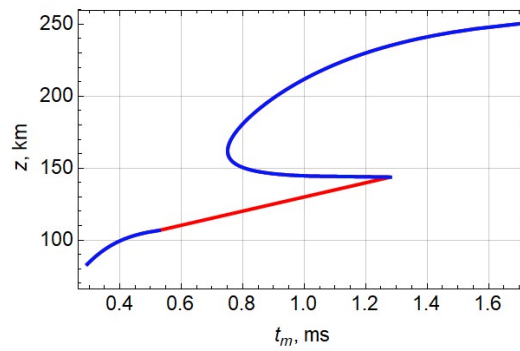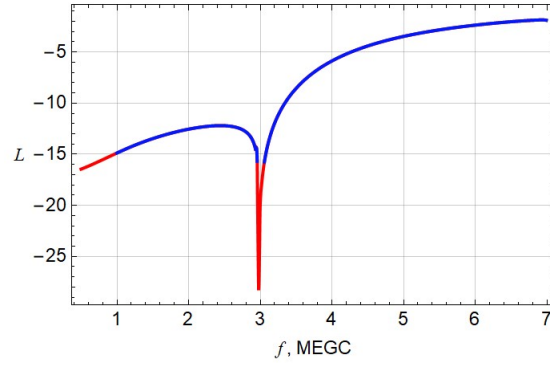
Fig. 12. Reflection height versus frequency.
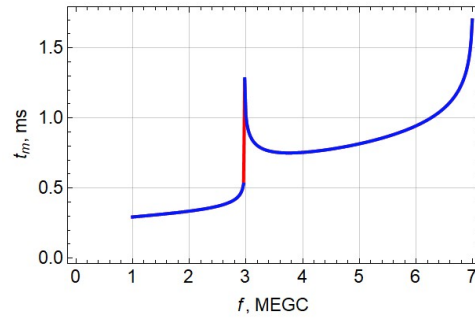
Fig. 13. Frequency dependence of the arrival time of the ray at the reflection point.

By eliminating the frequency f, a graph of the reflection height versus delay can be plotted (Figure 14) [18]. Finally, Figure 15 shows the dependence of the function L on frequency f [18].

**Fig. 14.** Reflection height versus delay.

Fig. 15. Logarithm of the amplitude function of frequency.

The simulation results are shown in Figures 16 and 17 [18]. The thick violet line shows the model dependence of the effective collision frequency on the height, and the thin green line shows the calculated values. It is seen that the model and calculated values for the lower ionosphere coincide with acceptable accuracy. This area is especially significant, since the main absorption of the radio wave is formed here.

In Figure 17, an extrapolation model is constructed from the calculated data (thin blue line). Obviously, at high frequencies, it needs to be corrected using chirp data.
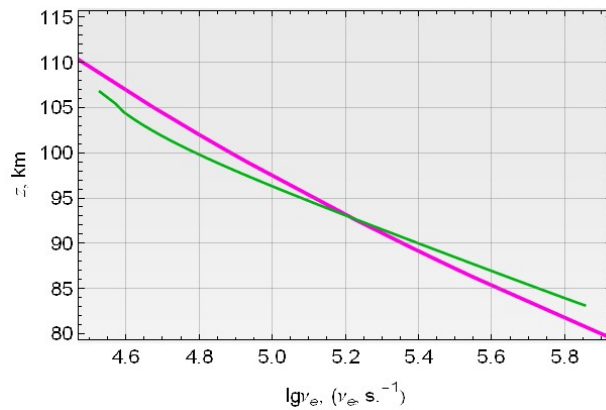
Fig. 16. Comparison of the dependence on the height of the model and calculated collision frequency.
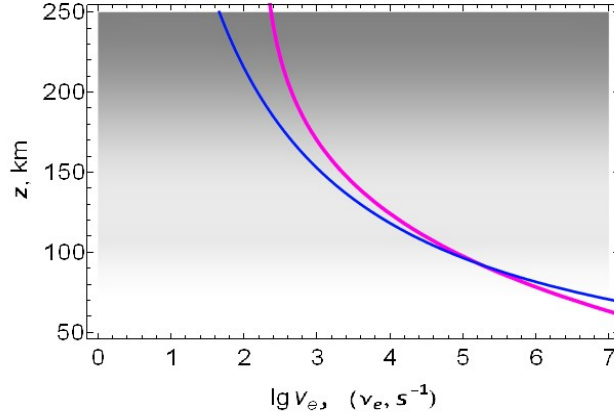
Fig. 17. Approximation of the effective collision frequency.

7 Conclusion

An algorithm is developed for studying the characteristics of frequency-modulated radio signals reflected from the ionosphere, which contains local plasma irregularities with low and high electron density [19]. Mathematical modeling of vertical sounding ionograms for various inhomogeneities both in the case of an ordinary wave and in the case of an extraordinary wave has been performed using a system of bicharacteristic equations.

In the material presented an algorithm for determining the polarization characteristics of the HF signal is given for the numerical simulating experiments on ionospheric inhomogeneities radiosounding. Since from the point of view of this approach the polarization characteristics are determined by the amplitude-phase relations of the interfering components, these characteristics are presented to sensitive instruments for recording and investigation local ionospheric inhomogeneities of various nature. Carrying out a large-scale model experiments of this kind for various models of inhomogeneities will allow us to identify typical frequency patterns for identifying features observed in experiments.

Thus, using the bicharacteristics method, an algorithm for recovering the effective frequency of collisions of electrons in the ionosphere was developed using data on signal attenuation during vertical sounding of the ionospheric plasma with a continuous frequency-modulated decameter signal. A numerical experiment has been carried out.

References

1. Davis, K.: Ionospheric Radio Waves, Blaisdell Publishing Company, Massachusetts–Toronto-London (1969).
2. Ipatov, E.B., Kryukovskii, A.S., Lukin, D.S., Palkin, E.A., Rastyagaev, D.V.: Methods of simulation of electromagnetic wave propagation in the ionosphere with allowance for the distributions of the electron concentration and the earths magnetic field. J. of Communications Technology and Electronics, 59(12), 1341-1348 (2014).
3. Kazantsev, A. N., Lukin, D.S., Spiridonov, Yu. G.: Method for studying of the radio waves propagation in an inhomogeneous magnetically active ionosphere. Space Researches, 5 (4), 593-600 (1967).
4. Lukin, D. S. and Spiridonov, Yu. G.: Application of the characteristics method for numerical solution of problems of radio wave propagation in an inhomogeneous and nonlinear medium. Radio Engineering and Electronics, 14 (9), 1673-1677 (1969).
5. Ginzburg, V. L.: Propagation of electromagnetic waves in plasma. Nauka, Moscow (1967).
6. Kryukovskii, A.S., Lukin, D.S., Kiryanova, K.S.: Method of extended bicharacteristic system in simulating wave propagation in ionospheric plasma. J. of Communications Technology and Electronics, 57 (9), 1039-1045 (2012).
7. Lukin, D.S., Palkin, E.A.: The numerical canonical method in the problems of diffraction and propagation of electromagnetic waves in inhomogeneous media. MIPT, Moscow (1982).
8. Bova, Yu. I., Kryukovsky, A. S., Lukin, D. S.: Propagation of Frequency-Modulated Electromagnetic Radiation in the Earth's Ionosphere with Allowance for Absorption and the External Magnetic Field. J. of Communications Technology and Electronics, 64 (1), 1-12 (2019).
9. Kryukovskii, A.S., Lukin, D.S., Rastyagaev, D.V., Skvortsova Y.I.: Mathematical simulation of propagation of frequency-modulated radio waves in ionospheric plasma. J. of Communications Technology and Electronics, 60 (10), 1049-1057 (2015).
10. Kryukovsky, A.S., Lukin D.S.: Concerning the field in the vicinity of a caustic cusp in ionospheric plasma layer. Radio Engineering and Electronic Physics, 26 (6), 1121-1126 (1981).
11. Kravtsov, Yu.A.: About one modification of the method of geometric optics. Izv. Universities (Radiophysics), 7 (4), 664–673 (1964).
12. Kryukovskii, A.S., Lukin, D.S.: Theoretical calculation of reference focal and diffractional electromagnetic fields based on wave catastrophe special functions. J. of Communications Technology and Electronics, 48 (8), 831-840 (2003).
13. Kiryanova, K.S., Kryukovsky, A.S.: Features of the ray propagation of radio waves in the Earth's ionosphere. T-Comm: Telecommunications and transport, 11, 25-28 (2012).
14. Karepov, S.L., Kryukovskii, A.S.: Calculation of a wave field using the method of local interpolating asymptotics. J. of Communications Technology and Electronics, 46(1), 34-40 (2001).
15. Kryukovskii, A.S.: Local uniform asymptotics of wave fields in the vicinity of basic and boundary cuspoidal caustics. J. of Communications Technology and Electronics, 41(1), 51-57 (1996).
16. Korotaev, V. V., Polarizing devices, Saint-Petersburg (2012).
17. Bova, Yu.I., Kryukovsky, A.S., Lukin, D.S., Rastyagaev, D.V.: Features of the effect of the Earth's ionosphere on the field of an ordinary wave in the vicinity of the caustic. Journal of Physics: Conference Series, 1632, 012005 (2020).
18. Kryukovsky, A.S., Lukin, D.S., Mikhaleva, E.V., Popchenko, O.V., Rastyagaev, D.V.: Diagnostics of the Effective Frequency of Electronic Collisions in the Ionosphere Based on

Analysis of the Amplitude Characteristics of Continuous Linear Frequency Modulated Radio Signals. In: 2020 7th All-Russian Microwave Conference (RMC), Moscow, Russia, 211-215 (2020).

19. Kryukovsky, A. S., Rastyagaev, D.V., Bova, Y.I., Popchenko, O.V.: Mathematical Simulation of the Ray Propagation of Frequency-Modulated Radio Signals in the Ionospheric Plasma in the Presence of Local Inhomogenies. In: 2020 7th All-Russian Microwave Conference (RMC), Moscow, Russia, 220-224 (2020).

20. Ipatov, E., Palkin, E., Rastyagaev, D.: Numerical Algorithm for LFM Signals Polarization Characteristics Simulation in Experiments on Inclined Radiosounding of Ionospheric Plasma Inhomogeneities. In: 2020 7th All-Russian Microwave Conference (RMC), Moscow, Russia, 216-219 (2020).